Transient aseismic vertical deformation across the Pisia-Skinos normal fault (Gulf of Corinth, Greece)

Zoë K. Mildon[1,*], Manuel Diercks[1], Gerald P. Roberts[2], Joanna P. Faure Walker[3], Athanassios Ganas[4], Ioannis Papanikolaou[5], Vassilis Sakas[6], Jenni Robertson[2], Claudia Sgambato[2], Sam Mitchell[4]

1. School of Geography, Earth and Environmental Sciences, University of Plymouth, Drake Circus, Plymouth, PL4 8AA, UK
2. School of Natural Sciences, Birkbeck, University of London, Malet Street, London, WC1E 7HX, UK
3. Institute for Risk and Disaster Reduction, University College London, Gower Street, London, WC1E 6BT, UK
4. Institute of Geodynamics, National Observatory of Athens, PO Box 20048, 11810, Athens, Greece
5. Laboratory of Mineralogy and Geology, Department of Natural Resources Development & Agricultural Engineering, Agricultural University of Athens, 11855 Athens, Greece.
6. Section of Geophysics and Geothermy, Department of Geology and Geoenvironment, National and Kapodistrian University of Athens, Panepistiomioupoli Zografou, 15784 Athens, Greece

* corresponding author: zoe.mildon@plymouth.ac.uk ORCID 0000-0001-6192-765X
Twitter handle: @ZoeMildon

Paper submitted to Geophysical Research Letters

Key points

- Spatial variations in vertical ground motion (uplift/subsidence) correlate with the mapped trace of the Pisia-Skinos fault in Greece.
- The ground deformation is non-uniform over the 6 years studied, and shows an up to 7x increase in rate, lasting at least 3 years.
- This transient interseismic deformation is hypothesised to be caused by shallow aseismic centimeter-scale slip on the Pisia-Skinos fault.

Abstract

Geodetically-derived deformation rates are sometimes used to infer seismic hazard, implicitly assuming that short-term (annual-decadal) deformation is representative of longer-term deformation. This is despite geological observations indicating that deformation/slip rates are variable over a range of timescales. Using geodetic data from 2016-2021, we observe an up to 7-fold increase in vertical deformation rate in mid-2019 across the Pisia-Skinos normal fault in Greece. We hypothesise that this deformation is aseismic as there is no temporally correlated increase in the earthquake activity (M>1). We explore four possible physical mechanisms, and our preferred hypothesis is that the transient deformation is caused by centimetre-scale slip in the upper 5km of the Pisia fault zone. Our results suggest that continental normal faults can exhibit variable deformation over shorter timescales than previously observed, and thus care should be taken when utilising geodetic rates to quantify seismic hazard.

Plain Language Summary

Slip rates of active faults are used in seismic hazard assessment to infer the frequency of damaging earthquakes. However slip rates are known to be variable when measured using different methodologies (e.g. geodesy, geomorphology) and timescales (years to millennia) for many types of faults in a range of tectonic settings. Hence we need to observe slip rates for different time scales and try to understand the mechanism(s) that cause slip rates to vary. In this paper, we present observations of vertical deformation around an active normal fault in the Gulf of Corinth, Greece. We see that the deformation is non-uniform during 2016-2021 (the time period of data availability), and we analyse the data to find that the

deformation rate increased in mid-2019. To try and understand the physical mechanism that may have caused this increase in deformation rate, we use simple modelling to test four different hypotheses. We find that the best fit to the observations is for centimetres of slip occurring on shallowest few kilometres of the fault. Our results highlight the importance of understanding short-term (annual-decadal) processes happening on active faults, and the potential pitfalls of using slip rates measured over short-timescales to infer seismic hazard.

Key Words

Tectonic deformation, normal faults, geodesy, seismic hazard, Greece

1. Introduction

Faults have been observed to have variable deformation and slip rates when measured over a wide range of timescales. Variations over timescales of thousands to millions of years are routinely studied using a variety of geological techniques, e.g. geological cross-sections (Ford et al., 2017) (Figure 1a), seismic reflection datasets (Lathrop et al., 2021; Meyer et al., 2002; Nixon et al., 2016), uplifted marine terraces (Roberts et al., 2009) (Figure 1b), ^{36}Cl cosmogenic dating of fault scarps (Benedetti et al., 2002; Cowie et al., 2017; Iezzi et al., 2021; Mechernich et al., 2018; Schlagenhauf et al., 2011) (Figure 1c). However, shorter term variations on the order of annual-decadal timescales are more challenging to study in the geological record due to their short-timescale and low preservation potential (Friedrich et al., 2003), instead geodesy can be used to study variable deformation on these timescales.

Short-term variations in deformation, detected using geodesy, have been observed across a range of tectonic settings, and we briefly summarise this herein. In convergent subduction zones, slow slip events (SSEs) have been observed, typically lasting weeks to months with slip rates from 0.001-1m/yr, with most occurring just downdip of the seismogenic zone (Schwartz & Rokosky, 2007). On the North Anatolian strike-slip fault, Rousset et al. (2016) identified a transient aseismic creep event, lasting one month, with slip of ~2cm occurring between 1-4km depth. These authors did not identify any external physical mechanism for this creep event, although they noted that there was no high rainfall anomaly, nor any significant local or teleseismic earthquakes during this time period. In extensional settings, transient deformation events lasting 2-4 years have been recognised in GPS data (Chamoli et al., 2014). The physical mechanism of these events is debated but may be related to a low angle normal fault or a megadetachment at mid to lower crustal depths of 15-30 km (Chamoli et al., 2014; Wernicke et al., 2008). Another example of transient deformation has been observed across a normal fault in the Delaware Basin, USA (Pepin et al., 2022), this deformation is inferred to be shallow (<5km depth) and related to fluid injection.

Given the variety of settings and timescales over which variable deformation and/or slip rate have been observed, an important question is how short-term (annual to decadal) transient deformation fits within the longer-term deformation of an individual fault, and therefore how the timescale of observation may affect our interpretation of the seismic hazard posed by an individual fault.

1.1 Extension on the Perachora peninsula, Gulf of Corinth, Greece

Extension in the Gulf of Corinth is taken up on a series of roughly E-W orientated normal faults (Figure 1d), the extension rate is 5.4-11mm/yr, constrained by GPS networks (Briole et al., 2021; Chousianitis et al., 2015; Clarke et al., 1998). On the Perachora peninsula, the main fault structures are the north-dipping Pisia and Skinos faults (Figure 1d). These faults form an en-echelon relay structure, with a separation of ~2km, they are hypothesised to be joined at depth due to their proximity and the pattern of converging slip vectors (Roberts, 1996).

In 1981 there was a sequence of three large earthquakes in the eastern Gulf of Corinth, occurring over a couple of weeks on the 24th and 25th February, and 4th March with magnitudes of M_w 6.7, 6.4 and 6.3 respectively (Figure 1a). The first two events occurred on the Pisia-Skinos fault and surface ruptures were mapped (Jackson et al., 1982; Roberts, 1996).

The most recent seismic activity in the eastern Gulf of Corinth was the 2020-2021 earthquake swarm (M<4) around the Perachora peninsula (Kapetanidis et al., 2023; Michas et al., 2022). The seismicity initially began at ~5km depth, and over time it deepened and propagated to the north-west/west, one hypothesis is that this sequence was triggered by fluid pressure changes induced by higher than average rainfall in the preceeding months (Michas et al., 2022).

Within the Gulf of Corinth, there are observations of variations in slip rates on the faults from thousands to millions of years (Figure 1a-c). Using onshore and offshore stratigraphy, it has been demonstrated that the Gulf of Corinth initiated at 5-4Ma and that the rate of extension has increased over time as the rift localised (Ford et al., 2017). Marine paleoshorelines in the footwall of the Pisia-Skinos fault have been uplifted over the last 300kyrs and show variable uplift rate over this time (Cooper et al., 2007; Roberts et al., 2009) (Figure 1b). In-situ cosmogenic ^{36}Cl analyses have been conducted on the Pisia-Skinos fault plane (Mechernich et al., 2018), and the resultant 30ka slip history shows variable slip rates (Figure 1c).

In this study, we present observations of shorter timescale variations in deformation rate across the Pisia-Skinos fault (Figure 2). Using InSAR measurements, we show that the rate of footwall uplift and hangingwall subsidence is non-uniform between 2016-2021 (Figure 2c). We test four different hypotheses for the causative mechanism, 1) shallow slip, 2) post-seismic after-slip, 3) interseismic slip on deep shear zones and 4) post-seismic visco-elastic rebound. We conclude that the most likely mechanism is shallow slip on the Pisia fault, and we infer that this deformation is aseismic based on the lack of temporally correlated earthquake activity. Our observation is the first example of short-term transient deformation on a normal fault driven by a shallow tectonic (i.e. non-human influenced) process. This has implications for understanding fault deformation and applications of geodesy to quantify seismic hazard.

2. Methods

2.1 Ground deformation data

The European Ground Motion Service (EGMS, https://egms.land.copernicus.eu/) is a ground deformation database, derived from Sentinel-1 satellite data (InSAR). Ideally N-S ground motions would be best to study the extension in the study area, however Sentinel-1 is insensitive to motions in this orientation due to side-looking satellites orbiting in a polar (i.e.

north-south) direction (Wright et al., 2004). Therefore, we focus on the vertical deformation across the active normal faults. On the Perachora peninsula, vertical deformation data is available over a 6-year time period (2016-2021). The deformation data are not spatially continuous as some data have been removed due to decorrelation effects. We avoid analysing data from these areas, and we focus our data analysis on areas with continuous data, as described below.

There is a clear discontinuity from uplift to subsidence, spatially correlated with the Pisia fault (Figure 2a), we analyse the vertical deformation in this area in two ways. Firstly, we construct a 9km north-south profile, approximately perpendicular to the fault trace, and take a 2km wide swath profile to create a cross-section of the uplift and subsidence. Secondly, we select two areas approximately 6x1.5km in the hangingwall and footwall of the fault (Figure 2a, areas 1&2). The area in the footwall of the fault is limited by the coastline, and therefore we selected a similar area on the hangingwall. We average the ground motions in these regions to create a time-series analysis of the deformation. Around the village of Kato Alepochori, there is an approximately 7x2km area of continuous uplift (Figure 2a, area 3). This region is in the footwall of the offshore section of the Skinos fault, therefore no information is available about hangingwall subsidence and thus we only take the average of the uplifting footwall ground motions.

The time-series datasets show non-uniform deformation rates (Figure 2c). Firstly we calculate the differential vertical motion between the two areas around Perachora, and then we apply a piecewise linear regression (Pilgrim, 2021) to constrain the date that the deformation rate increases.

Finally, we compare the time-series datasets to earthquake activity, which is taken from the NOA earthquake database (https://www.gein.noa.gr/en/services-products/database-search/, date accessed 01/06/2023, for 20km radius circular area around 38.035°N 22.925°E, close to Perachora), we calculate the cumulative number of earthquakes and seismic moment released for earthquakes M>1 from 2016-2021 and compare this to the deformation time-series (Figure 2d).

2.2 Modelling of hypothesised tectonic processes

We test four hypotheses of the causative physical mechanism of the transient vertical deformation signal observed in the EGMS data. For one hypothesis (shallow after-slip), we use field observations. For three hypotheses (detailed below), we use simple modelling to assess likely hypotheses, note that we do not seek to do a full inversion of the vertical deformation data given the spatial discontinuity along the length of the Pisia-Skinos fault.

2.2.1 Shallow slip and interseismic (shear zone) slip

To model vertical deformation associated with shallow slip or interseismic slip on a deep shear zone, we use an elastic half-space model in Coulomb 3.4 (Toda et al., 2005). We model a simplified fault 10km long with strike/dip/rake of 270°/60°/-90°. For modelling shallow slip, we test uniform slip over a range of different depths, down to a maximum of 5 km depth based on the onset of seismicity during the 2020-2021 earthquake sequence (Michas et al., 2022). For modelling interseismic slip, we model the slipping area between 15-24km depth (following a similar approach from the Italian Apennines (Cowie et al., 2013; Mildon et al., 2022)) at a representative rate of 1mm/yr. We resolve the vertical deformation at 0.1km depth (Figure 3ai and bi), as this is the minimum depth allowed in the software. We compare N-S profiles through the modelled data and the actual data (Figure 3aii and bii).

2.2.2 Post-seismic deformation

We used PSGRN/PSCMP (Wang et al., 2006) to model post-seismic deformation patterns for 35-40 years after the 1981 earthquake sequence. We use a simplified fault model (length 15km, strike/dip/rake as above) to generate an earthquake with a comparable magnitude to the largest of the 1981 earthquakes (M_w=6.7). We use a simple three layer rheological model; 1) brittle crust from 0-16.5km, Vp=5.8km/s, density 2600kg/m^3, eta=0PaS (the steady-state viscosity); 2) lower crust from 16.5-30km, Vp=6.7km/s, density=2800kg/m^3, eta=6 x 10^{16}PaS; 3) mantle below 30km, Vp=8km/s, density=3300kg/m^3 and eta=1 x 10^{18}PaS, for all layers, Vp/Vs=1.8 (Figure 3cii). This rheological model is based on multiple publications from Greece (Clément et al., 2004; Janský et al., 2007; Sachpazi et al., 2007; Westaway, 2002; Zelt et al., 2005). Again, we resolve the vertical deformation at 0.1km depth (Figure 3c).

3. Results

In map view, there is a transition from uplift to subsidence coincident with the Pisia-Skinos fault, especially around the village of Perachora (Figure 2a). On the N-S vertical deformation profile (Figure 2b), there is a clear transition from uplift to subsidence coincident with the surface trace of the Pisia fault. Taking the average across the swath of data, the maximum 6-year averaged rate of uplift and subsidence across the N-S profile are 1.4mm/yr and -4mm/yr respectively.

Two of the selected areas are undergoing uplift, the 6-year (2016-2021) averaged uplift rate around Perachora is 0.92±0.01mm/yr and around Alepochori it is 0.93±0.01mm/yr (Figure 2c). While these uplift rates are similar, for the majority of the time series, the Alepochori region has higher uplift rates than the Perachora region, which may be expected because the Alepochori region is closer to the centre of the Pisia-Skinos fault.

The 6-year averaged subsidence rate for the analysed area on Perachora is -2.60±0.05mm/yr, this is ~3 times higher than the uplift rate in the corresponding footwall region (Figure 2c).

The vertical deformation rate is not uniform over the time interval studied. Assuming that there is a single breakpoint (ie a single time point where the deformation rate increases), the results of the piecewise linear regression analysis on the differential vertical motion around Perachora gives that the change in deformation rate occurs at 07/08/2019 (± 6 days) (Figure S1). Interpreting the GPS baseline data using this date also results in an increase in deformation rate (Figure 2e), although the magnitude of increase is smaller, perhaps because the baseline is not perpendicular to the fault trace (Figure 1d). We interpret that the deformation before 07/08/2019 is representative of steady-state, whereas the deformation after 07/08/2019 represents a transient phase. We then calculate the uplift/subsidence rates for before and after this date using linear regression (Figure 2c). In the Perachora region, the deformation rate increases by a factor of 5-7. The increase in uplift rate is lower in the Alepochori region, where it increases by a factor of ~2.

At the date we have inferred an increase in the deformation rate (07/08/2019), there is no temporally correlated increase in either the cumulative number of earthquakes, nor the cumulative moment released (Figure 2d). Therefore we interpret that the increase in deformation rate is aseismic, or at least any seismic energy released is small and below the detection threshold of seismometers (M<1).

4. Modelling of hypothesised causative process

We hypothesise that there are four possible tectonic mechanisms which could explain the signal we observe across the Perachora peninsula: shallow slip, post-seismic slip, interseismic slip on deep shear zones, or post-seismic visco-elastic rebound. We have investigated each of these hypotheses using simple models; we do not seek to invert the data fully, but instead to understand which section of the fault may be slipping.

4.1 Shallow slip

Looking at the N-S profile across the Perachora peninsula (Figure 2b), the wavelength of the subsidence is ~7km, which suggests that the underlying physical mechanism is likely to be occurring in the upper few kilometres of the crust.

Using an elastic half-space model (Coulomb 3.4 (Toda et al., 2005)), we tested slip over a range of depths (down to 5km), fault dips and slip magnitudes (Figure S2) and compared the shape and size of the resulting deformation pattern perpendicular to the fault. From our modelling, the following points emerge; 1) slip does not reach the surface, as this would produce an asymmetric subsidence signal which would not match the observations; 2) the dip and depth of slip affect the width and magnitude of the subsidence signal and therefore there is a trade-off between these two factors; and 3) the magnitude of slip directly affects the magnitude of the resulting vertical deformation, and seems to have little impact on the shape of the uplift/subsidence. The best-fit simple model to the N-S profile has the fault slipping 1.8cm from 2-4km depth (Figure 3a), and while this is not a full inversion, this gives an indication of the approximate depth and magnitude of slip required to produce the observed signal. Given that there is no temporally coincident increase in earthquake activity (Figure 2d), we suggest that this slip must be aseismic. We believe this is the first such observation of a transient shallow slip event on a normal fault globally that cannot be linked to human activities.

Our model may provide an alternative explanation for triggering of the 2020 earthquake swarm, as shallow slip in mid-2019 would transfer stress downwards and thus triggering the shallowest earthquakes in 2020 at 5km depth. We do not suggest that the shallow slip was triggered by meteoric fluids because the increase in deformation rate began before the period of high rainfall (Michas et al., 2022).

4.2 Post-seismic after-slip

There are several observations of surficial after-slip occurring after large normal faulting earthquakes, for example the 2009 Mw=6.3 L'Aquila earthquake (D'Agostino et al., 2012; Wilkinson et al., 2010, 2012), the 2020 Mw=7.0 Samos earthquake (Ganas et al., 2021), the 1980 Ms=6.9 Irpinia earthquake (Ascione et al., 2020) and the 2006 Mw=7.0 Mozambique earthquake (Copley et al., 2012). In all these examples, the after-slip is interpreted to be 'filling in' coseismic slip deficits, and it is observed days to months after the large earthquake and it decays over time.

After the 1981 earthquake on the Pisia-Skinos fault, the coseismic slip was measured from surface ruptures at a clear piercing point (Figure 3b) which is close to the N-S profile taken through the data. This has been repeatedly measured over the subsequent years by the authors at this exact point, firstly in 2001 (Roberts et al., 2009) and most recently in May 2023, and this measurement has not changed (within an estimated error of ±0.5cm). Therefore, we discount post-seismic after-slip as the causal mechanism because it is not consistent with 1) our observations of an acceleration 35 years after the 1981 earthquake and 2) that the offset across the surface rupture has not increased.

4.3 Interseismic slip on lower crustal shear zones

Our elastic-halfspace model of slip on an underlying deep shear zone replicates the uplift/subsidence transition spatially coincident with the fault trace (Figure 3c). However, the N-S wavelength of the subsidence signal (~30km) is far larger than our observations (~7km wavelength), this due to the modelled slip occurring on the deep shear zone.

Furthermore, the vertical deformation is two orders of magnitude smaller than our observations, and therefore we discount this physical mechanism.

4.4 Post-seismic visco-elastic rebound

Using PSGRN/PSCMP (Wang et al., 2006) we calculate the post-seismic vertical deformation at 35 and 40 years for M 6.7 earthquake and then calculate the difference to get the vertical deformation rate. The model shows that there would be subsidence everywhere around the fault, including in the footwall (Figure 3d). Our observations do not agree with this pattern, and hence we discount this physical mechanism.

5. Discussion

5.1. Implications for fault behaviour

From our study, we are unable to determine a trigger for the transient phase of deformation and the hypothesised mechanism of aseismic slip on the fault plane, however we can speculate on the possible triggers. We have assumed that both the steady-state and transient deformation phases can be fit by linear regression, however by visually inspecting the fit to differential motion time-series (Figure S1), the transient deformation may be better fit using a non-linear regression, e.g. exponential or a second-order polynomial. This suggests that the underlying physical mechanism may be a non-linear process.

The rate-and-state friction framework is commonly applied to earthquake behaviour, based on laboratory experiments and numerical modelling. One question is whether aseismic slip and/or transient deformation is possible within a rate and state framework, and several studies using numerical modelling show that aseismic slip can occur between seismic slip (ie earthquakes). The mechanism within rate and state causing transient slip periods is debated, some authors hypothesise that the stability of the fault is related to the length of the fault (Biemiller & Lavier, 2017; Rubin, 2008). Whereas other studies hypothesise that transient slip occurs due to variations in fault zone rheology, either by observing transient slip occurring at rheological transitions (Lapusta & Liu, 2009; Liu & Rice, 2005), or by varying the proportions of velocity-weakening and -strengthening material (Skarbek et al., 2012). The fault geometry utilised in these studies is variable, but one study is based on a normal fault. In this study (Biemiller & Lavier, 2017), the authors model a normal fault with a shallow (~5km) velocity-weakening zone. Their models show both aseismic slip transients and clustered earthquakes, with the aseismic transients accommodating 15-20cm slip per event over 5-25 years – these modelled events are not dissimilar in magnitude to our observations. Some studies find that variable seismic/aseismic slip can occur at low effective stresses (Rubin, 2008; Skarbek et al., 2012), ie at shallow depths or areas with high pore fluid pressure. While we do not know the pore fluid pressure at depth, our best fit model of slip occurring in the upper 5km would imply low effective stresses.

Therefore, perhaps the transient deformation we observe, and the shallow slip we hypothesise is allowed within a typical rate-and-state framework for a continental fault (ie not a subduction zone). Of the hypothesised causative mechanisms for variable fault behaviour, we suggest that variability in the fault zone rheology is more likely, as the length of the fault is unlikely to change on the studied timescales This hypothesis could be investigated further by drilling and collecting samples from the fault plane at the inferred depth of the deformation, i.e., 2-4km depth.

5.2 Implications for utilising geodetically derived rates in seismic hazard assessment

Our observation raises important questions about how short-term (annual-decadal) deformation rates relate to longer-term deformation rates. By splitting the time-series datasets into steady-state motion and transient signal, we can compare these rates and link them to independent longer term uplift records from the Perachora coastline to estimate how frequently transient periods of deformation may occur.

We hypothesise that the long-term uplift in the Perachora coastal area is a combination of coseismic uplift, steady state, and transient uplift. The long-term uplift rate is 0.51mm/yr over 125kyrs (Cooper et al., 2007; Roberts et al., 2009). The coseismic uplift in 1981 at the coastline was 10cm (Cooper et al., 2007) and we use a recurrence interval of 0.9-1.3kyrs (Mechernich et al., 2018) to calculate the total of coseismic uplift over 125kyrs. The steady state rate is taken to be 0.39mm/yr (Figure 2c). The transient deformation has been ongoing for at least 2.5yrs, so we assume a range of durations (3-10yrs) for our simple approach to calculating the recurrence interval of transient deformation periods. Considering the uncertainties on earthquake recurrence interval and our assumed 3-10yr transient duration, we calculate that the transient recurrence is in the range of ~110-1800yrs. While this is a large range, what it does imply is that the minimum expected transient recurrence is greater than the time that high-resolution satellite-based geodesy has been available. Therefore, it is perhaps not surprising that similar transients have not been previously observed in this region, and the limited examples from elsewhere in the world.

Assuming other faults globally behave like the Pisia-Skinos fault and experience transient phases, this may help to explain why there are sometimes discrepancies between geodetic and geologic rates of deformation. This also highlights a potential pitfall of using short-term geodetic deformation rates, as the inferred seismic hazard would be different using the steady-state versus transient rates we calculate. Therefore, this study highlights the need to understand how faults deform over short timescales, from years to thousands of years.

5. Conclusions

Using geodetic data we observe vertical deformation (uplift and subsidence) which spatially correlates with the mapped fault trace of the Pisia-Skinos normal fault in the Gulf of Corinth, Greece. By studying the time-series of the vertical deformation, we can see that this deformation is not uniform over the 6-year time period, and instead there is a 5-7-fold increase in deformation rate in mid-2019. Using simple elastic models, we explore four possible tectonic mechanisms that could explain the spatial pattern of the deformation, and we hypothesise that the most likely explanation is that the vertical deformation is caused by small amounts (~1-2cm) of shallow (~2-4km depth) transient slip on the Pisia-Skinos fault. We use the interpreted steady-state and transient rate to infer how frequently such transient episodes could occur. Our study highlights a potential pitfall of using geodetically-derived deformation rates to inform seismic hazard, as it may be difficult to determine whether a geodetic rate is truly representative of 'steady state' or whether a transient phase has been captured. This highlights that the occurrence of short-term (annual-decadal) transient phases of deformation merits further investigation.

Data availability statement

GPS 30-s data (daily files) are made available by Hexagon Smart Net Greece for academic use. EGMS data are available free of charge by https://land.copernicus.eu/pan-european/european-ground-motion-service.

Acknowledgements

This study was funded by NERC Standard Grant (NE/V012894/1, PI – G. Roberts) and UKRI Future Leaders Fellowship (MR/T041994/1, PI – Z. Mildon). M. Diercks is supported by the University of Plymouth, School of Geography, Earth and Environmental Sciences PhD studentship. Spatial analysis and figures made using QGIS v3.16. We thank the Hexagon Smart Net Greece for releasing their GPS data to A. Ganas.

Figures

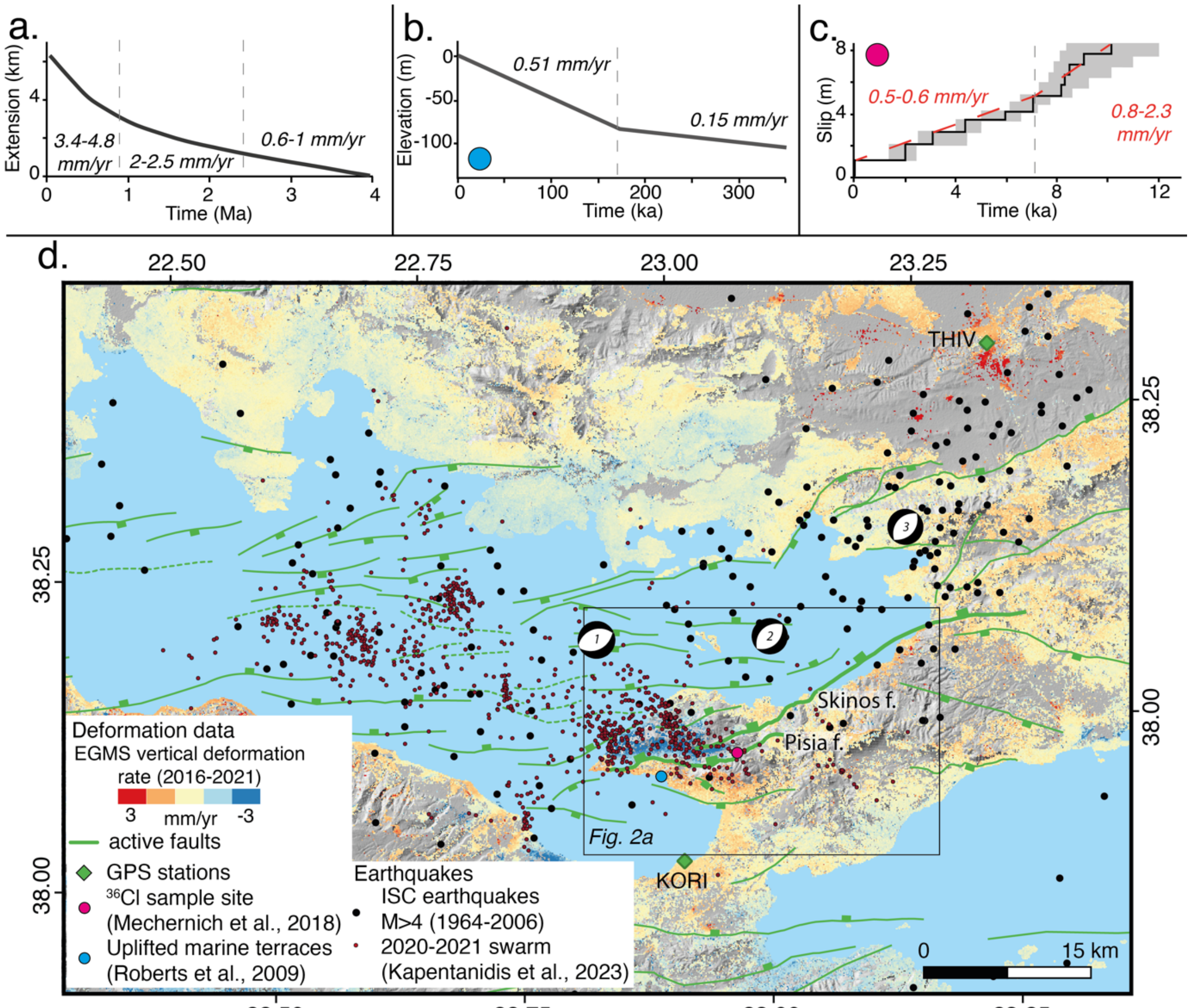

Figure 1 – Overview of the scientific basis and study region. a. Evidence for variation in extension rate across the western Gulf of Corinth over millions of years (Ford et al., 2017)*. b. Evidence for variation in the uplift rate of the southern Perachora coastline (footwall of the Pisia-Skinos fault) from dated marine terraces* (Roberts et al., 2009)*. c. Evidence for variation in slip rate on the Pisia fault, inverted from ^{36}Cl cosmogenic analyses* (Mechernich et al., 2018)*. d. Summary map of the study area, showing the active faults, vertical deformation dataset, and recorded earthquakes. Focal mechanisms are for the 1981 sequence, 1-24/3/1981, M6.7, 2-25/3/1981, M6.4, 3-4/3/1981, M6.3. Map units are in latitude and longitude. The box shows the location of Figure 2a.*

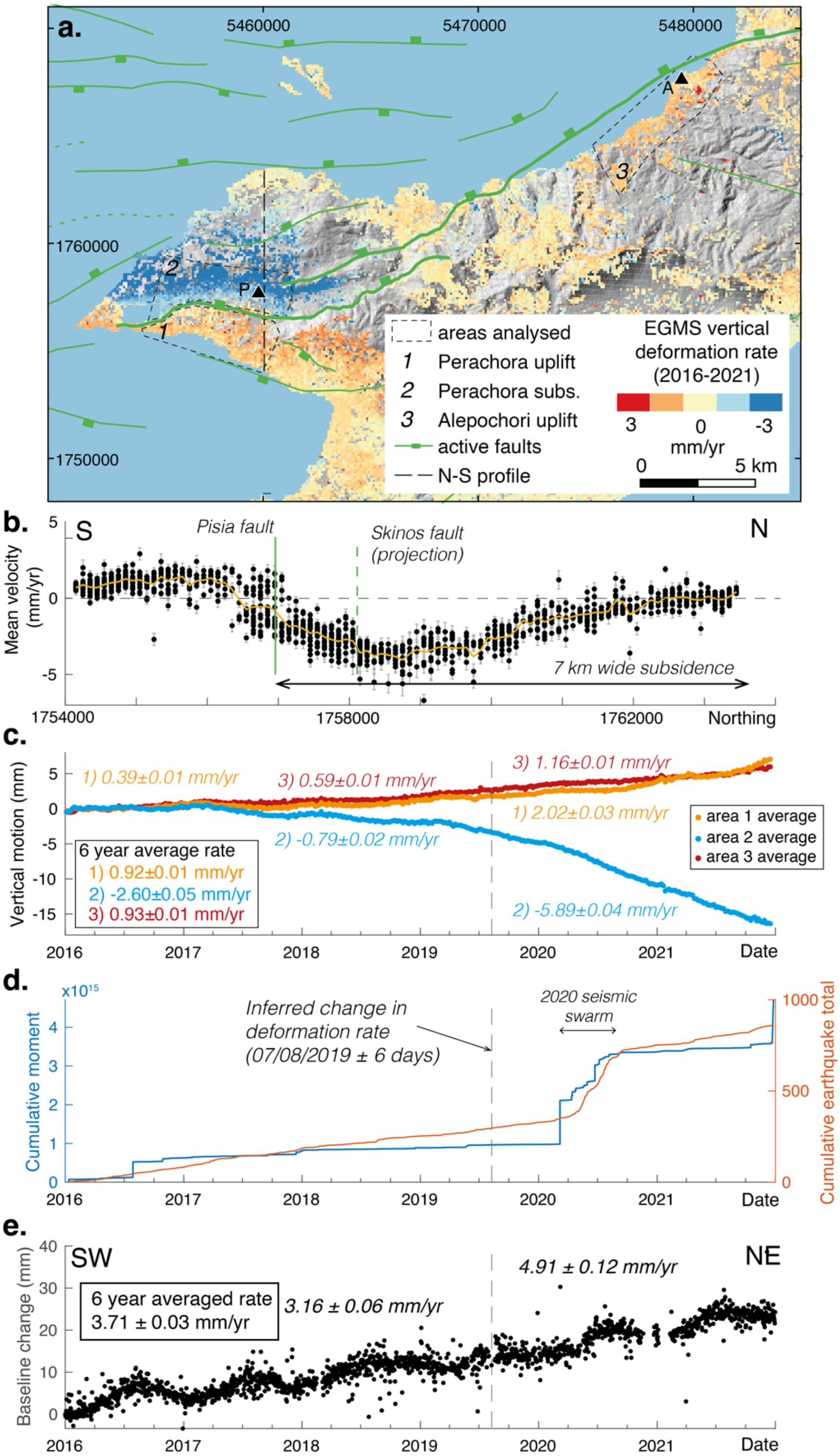

Figure 2 – Deformation data from the Perachora peninsula. a. Map of the region showing the spatial pattern of the EGMS vertical deformation, map coordinates are ETRS89-LAEA Europe. Three small regions are analysed in detail where there is good data consistency and coverage. Towns are as follows, P-Perachora, A-Alepochori. b. Mean rate of vertical deformation along a 2km wide N-S profile across the Pisia fault. Error bars are standard

deviation reported by the EGMS. c. Time series of the three regions analysed. Rates and associated errors are calculated using linear regression after filtering out the seasonal signal. Rates given in italics are for before/after the inferred increase in deformation rate at 07/08/2019. d. Earthquake activity over the time interval studied. e. Time-series of GPS baseline change between two stations (see Figure 1d for locations). An increase in rate can also be interpreted at the same time as that interpreted from the EGMS data.

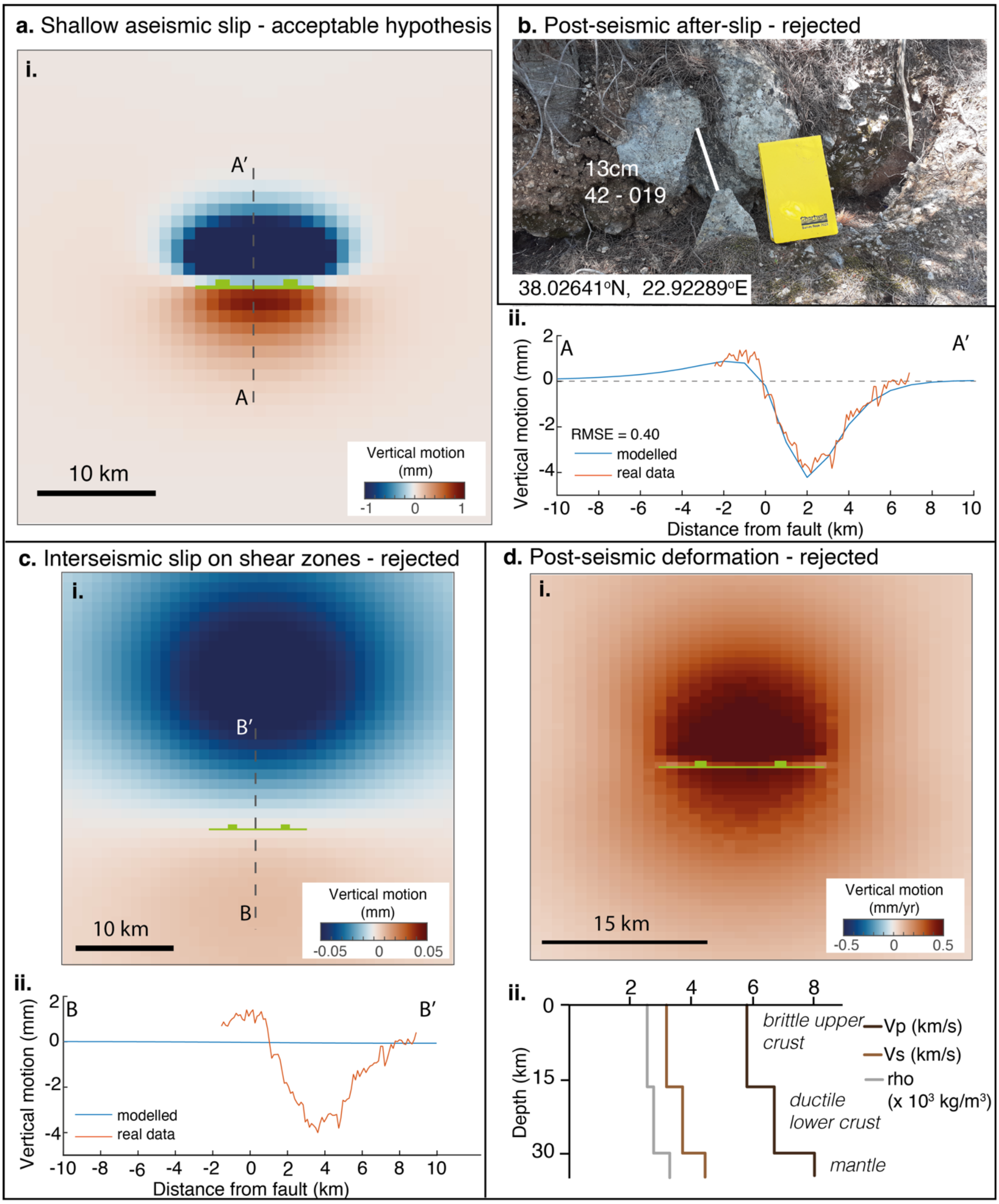

Figure 3 – Possible tectonic mechanisms for the vertical deformation observed across the Pisia fault. a. Shallow slip, our model (i) has the fault slipping 1.8cm from 2-4km depth, comparing the modelled deformation to the N-S profile (ii) there is good agreement with the shape and magnitude of the actual data. This is our preferred hypothesis to explain the observed deformation. b. Photo of the 1981 surface rupture, showing no evidence for post-seismic after-slip, as the offset is the same (with measurement error of ±0.5cm) as previous observations. c. Interseismic slip on deep underlying shear zones, our model (i) matches the

uplift/subsidence pattern, but the wavelength of the subsidence signal is far larger than observed and the deformation is an order of magnitude smaller (ii). d. Post-seismic visco-elastic rebound, our model (i) implies uplift in both the footwall and hangingwall, which does not match the observations. ii shows the rheological model used.

References

Ascione, A., Nardò, S., & Mazzoli, S. (2020). The MS 6.9, 1980 Irpinia Earthquake from the Basement to the Surface: A Review of Tectonic Geomorphology and Geophysical Constraints, and New Data on Postseismic Deformation. *Geosciences*, *10*(12), 493. https://doi.org/10.3390/geosciences10120493

Benedetti, L., Finkel, R., Papanastassiou, D., King, G., Armijo, R., Ryerson, F., et al. (2002). Post-glacial slip history of the Sparta fault (Greece) determined by 36Cl cosmogenic dating: Evidence for non-periodic earthquakes. *Geophysical Research Letters*, *29*(8), doi: 10.1029/2001GL014510. https://doi.org/10.1029/2001GL014510

Biemiller, J., & Lavier, L. (2017). Earthquake supercycles as part of a spectrum of normal fault slip styles. *Journal of Geophysical Research: Solid Earth*, *122*(4), 3221–3240. https://doi.org/10.1002/2016JB013666

Briole, P., Ganas, A., Elias, P., & Dimitrov, D. (2021). The GPS velocity field of the Aegean. New observations, contribution of the earthquakes, crustal blocks model. *Geophysical Journal International*, *226*(1), 468–492. https://doi.org/10.1093/gji/ggab089

Chamoli, A., Lowry, A. R., & Jeppson, T. N. (2014). Implications of transient deformation in the northern Basin and Range, western United States. *Journal of Geophysical Research: Solid Earth*, *119*(5), 4393–4413. https://doi.org/10.1002/2013JB010605

Chousianitis, K., Ganas, A., & Evangelidis, C. P. (2015). Strain and rotation rate patterns of mainland Greece from continuous GPS data and comparison between seismic and geodetic moment release. *Journal of Geophysical Research: Solid Earth*, *120*(5), 3909–3931. https://doi.org/10.1002/2014JB011762

Clarke, P. J., Davies, R. R., England, P. C., Parsons, B., Billiris, H., Paradissis, D., et al. (1998). Crustal strain in central Greece from repeated GPS measurements in the interval 1989-1997. *Geophysical Journal International*, *135*(1), 195–214. https://doi.org/10.1046/j.1365-246X.1998.00633.x

Clément, C., Sachpazi, M., Charvis, P., Graindorge, D., Laigle, M., Hirn, A., & Zafiropoulos, G. (2004). Reflection–refraction seismics in the Gulf of Corinth: hints at deep structure and control of the deep marine basin. *Tectonophysics*, *391*(1), 97–108. https://doi.org/10.1016/j.tecto.2004.07.010

Cooper, F. J., Roberts, G. P., & Underwood, C. J. (2007). A comparison of 103–105 year uplift rates on the South Alkyonides Fault, central Greece: Holocene climate stability and the formation of coastal notches. *Geophysical Research Letters*, *34*(14). https://doi.org/10.1029/2007GL030673

Copley, A., Hollingsworth, J., & Bergman, E. (2012). Constraints on fault and lithosphere rheology from the coseismic slip and postseismic afterslip of the 2006 Mw7.0 Mozambique earthquake. *Journal of Geophysical Research: Solid Earth*, *117*(3), 1–16. https://doi.org/10.1029/2011JB008580

Cowie, P. A., Scholz, C. H., Roberts, G. P., Faure Walker, J. P., & Steer, P. (2013). Viscous roots of active seismogenic faults revealed by geologic slip rate variations. *Nature Geoscience*, *6.12*(November), 1036–1040. https://doi.org/10.1038/ngeo1991

Cowie, P. A., Phillips, R. J., Roberts, G. P., McCaffrey, K. J. W., Zijerveld, L. J. J., Gregory, L. C., et al. (2017). Orogen-scale uplift drives episodic behaviour of earthquake faults. *Nature Scientific Reports*, (November 2016), 1–10. https://doi.org/10.1038/srep44858

D'Agostino, N., Cheloni, D., Fornaro, G., Giuliani, R., & Reale, D. (2012). Space-time distribution of afterslip following the 2009 L'Aquila earthquake. *Journal of Geophysical Research: Solid Earth*, *117*(2), 1–23. https://doi.org/10.1029/2011JB008523

Ford, M., Hemelsdaël, R., Mancini, M., & Palyvos, N. (2017). Rift migration and lateral propagation: evolution of normal faults and sediment-routing systems of the western Corinth rift (Greece). *Geological Society, London, Special Publications*, *439*(1), 131–168. https://doi.org/10.1144/SP439.15

Friedrich, A. M., Wernicke, B. P., Niemi, N. A., Bennett, R. A., & Davis, J. L. (2003). Comparison of geodetic and geologic data from the Wasatch region, Utah, and implications for the spectral character of Earth deformation at periods of 10 to 10 million years. *Journal of Geophysical Research: Solid Earth*, *108*(B4). https://doi.org/10.1029/2001JB000682

Ganas, A., Elias, P., Briole, P., Valkaniotis, S., Escartin, J., Tsironi, V., et al. (2021). Co-seismic and post-seismic deformation, field observations and fault model of the 30 October 2020 Mw = 7.0 Samos earthquake, Aegean Sea. *Acta Geophysica*, *69*(3), 999–1024. https://doi.org/10.1007/s11600-021-00599-1

Iezzi, F., Roberts, G., Faure Walker, J., Papanikolaou, I., Ganas, A., Deligiannakis, G., et al. (2021). Temporal and spatial earthquake clustering revealed through comparison of millennial strain-rates from 36Cl cosmogenic exposure dating and decadal GPS strain-rate. *Scientific Reports*, *11*(1), 23320. https://doi.org/10.1038/s41598-021-02131-3

Jackson, J. A., Gagnepain, J., Houseman, G., King, G. C. P., Papadimitriou, P., Soufleris, C., & Virieux, J. (1982). Seismicity, normal faulting, and the geomorphological development of the Gulf of Corinth (Greece): the Corinth earthquakes of February and March 1981. *Earth and Planetary Science Letters*, *57*(2), 377–397. https://doi.org/10.1016/0012-821X(82)90158-3

Janský, J., Plicka, V., Lyon-Caen, H., & Novotný, O. (2007). Estimation of velocity in the uppermost crust in a part of the western Gulf of Corinth, Greece, from the inversion of P and S arrival times using the neighbourhood algorithm. *Journal of Seismology*, *11*(2), 199–204. https://doi.org/10.1007/s10950-007-9047-1

Kapetanidis, V., Michas, G., Spingos, I., Kaviris, G., & Vallianatos, F. (2023). Cluster Analysis of Seismicity in the Eastern Gulf of Corinth Based on a Waveform Template Matching Catalog. *Sensors*, *23*(6), 2923. https://doi.org/10.3390/s23062923

Lapusta, N., & Liu, Y. (2009). Three-dimensional boundary integral modeling of spontaneous earthquake sequences and aseismic slip. *Journal of Geophysical Research: Solid Earth*, *114*(B9). https://doi.org/10.1029/2008JB005934

Lathrop, B. A., Jackson, C. A. -L., Bell, R. E., & Rotevatn, A. (2021). Normal Fault Kinematics and the Role of Lateral Tip Retreat: An Example From Offshore NW Australia. *Tectonics*, *40*(5). https://doi.org/10.1029/2020TC006631

Liu, Y., & Rice, J. R. (2005). Aseismic slip transients emerge spontaneously in three-dimensional rate and state modeling of subduction earthquake sequences. *Journal of Geophysical Research: Solid Earth*, *110*(B8). https://doi.org/10.1029/2004JB003424

Mechernich, S., Schneiderwind, S., Mason, J., Papanikolaou, I. D., Deligiannakis, G., Pallikarakis, A., et al. (2018). The Seismic History of the Pisia Fault (Eastern Corinth Rift, Greece) From Fault Plane Weathering Features and Cosmogenic 36Cl Dating. *J. Geophys. Res. Solid Earth*, *123*(5), 4266–4284. https://doi.org/10.1029/2017JB014600

Meyer, V., Nicol, A., Childs, C., Walsh, J. J., & Watterson, J. (2002). Progressive localisation of strain during the evolution of a normal fault population. *Journal of Structural Geology*, *24*(8), 1215–1231. https://doi.org/10.1016/S0191-8141(01)00104-3

Michas, G., Kapetanidis, V., Spingos, I., Kaviris, G., & Vallianatos, F. (2022). The 2020 Perachora peninsula earthquake sequence (East Corinth Rift, Greece): spatiotemporal evolution and implications for the triggering mechanism. *Acta Geophysica*, *70*(6), 2581–2601. https://doi.org/10.1007/s11600-022-00864-x

Mildon, Z. K., Roberts, G. P., Faure Walker, J. P., Beck, J., Papanikolaou, I., Michetti, A. M., et al. (2022). Surface faulting earthquake clustering controlled by fault and shear-zone interactions. *Nature Communications*, *13*(1), 7126. https://doi.org/10.1038/s41467-022-34821-5

Nixon, C. W., McNeill, L. C., Bull, J. M., Bell, R. E., Gawthorpe, R. L., Henstock, T. J., et al. (2016). Rapid spatiotemporal variations in rift structure during development of the Corinth Rift, central Greece. *Tectonics*, *35*(5), 1225–1248. https://doi.org/10.1002/2015TC004026

Pepin, K. S., Ellsworth, W. L., Sheng, Y., & Zebker, H. A. (2022). Shallow Aseismic Slip in the Delaware Basin Determined by Sentinel-1 InSAR. *Journal of Geophysical Research: Solid Earth*, *127*(2), e2021JB023157. https://doi.org/10.1029/2021JB023157

Pilgrim, C. (2021). piecewise-regression (aka segmented regression) in Python. *Journal of Open Source Software*, *6*(68), 3859. https://doi.org/10.21105/joss.03859

Roberts, G. P. (1996). Noncharacteristic normal faulting surface ruptures from the Gulf of Corinth, Greece. *Journal of Geophysical Research*, *101*, 25255–25267.

Roberts, G. P., Houghton, S. L., Underwood, C., Papanikolaou, I., Cowie, P. A., van Calsteren, P., et al. (2009). Localization of Quaternary slip rates in an active rift in 10 5 years: An example from central Greece constrained by 234 U- 230 Th coral dates from uplifted paleoshorelines. *J. Geophys. Res.*, *114*(B10), B10406. https://doi.org/10.1029/2008JB005818

Rousset, B., Jolivet, R., Simons, M., Lasserre, C., Riel, B., Milillo, P., et al. (2016). An aseismic slip transient on the North Anatolian Fault. *Geophysical Research Letters*, *43*(7), 3254–3262. https://doi.org/10.1002/2016GL068250

Rubin, A. M. (2008). Episodic slow slip events and rate-and-state friction. *Journal of Geophysical Research: Solid Earth*, *113*(B11). https://doi.org/10.1029/2008JB005642

Sachpazi, M., Galvé, A., Laigle, M., Hirn, A., Sokos, E., Serpetsidaki, A., et al. (2007). Moho topography under central Greece and its compensation by Pn time-terms for the accurate location of hypocenters: The example of the Gulf of Corinth 1995 Aigion earthquake. *Tectonophysics*, *440*, 53–65. https://doi.org/10.1016/j.tecto.2007.01.009

Schlagenhauf, A., Manighetti, I., Benedetti, L., Gaudemer, Y., Finkel, R., Malavieille, J., & Pou, K. (2011). Earthquake supercycles in Central Italy, inferred from 36Cl exposure dating. *Earth and Planetary Science Letters*, *307*(3–4), 487–500. https://doi.org/10.1016/j.epsl.2011.05.022

Schwartz, S. Y., & Rokosky, J. M. (2007). Slow slip events and seismic tremor at circum-Pacific subduction zones. *Reviews of Geophysics*, *45*(3). https://doi.org/10.1029/2006RG000208

Skarbek, R. M., Rempel, A. W., & Schmidt, D. A. (2012). Geologic heterogeneity can produce aseismic slip transients. *Geophysical Research Letters*, *39*(21). https://doi.org/10.1029/2012GL053762

Toda, S., Stein, R. S., Richards-Dinger, K., & Bozkurt, S. B. (2005). Forecasting the evolution of seismicity in southern California: Animations built on earthquake stress transfer. *Journal of Geophysical Research*, *110*(B5), B05S16. https://doi.org/10.1029/2004JB003415

Wang, R., Lorenzo-Martín, F., & Roth, F. (2006). PSGRN/PSCMP - A new code for calculating co- and post-seismic deformation, geoid and gravity changes based on the viscoelastic-gravitational dislocation theory. *Computers and Geosciences*, *32*(4), 527–541. https://doi.org/10.1016/j.cageo.2005.08.006

Wernicke, B., Davis, J. L., Niemi, N. A., Luffi, P., & Bisnath, S. (2008). Active megadetachment beneath the western United States. *Journal of Geophysical Research: Solid Earth*, *113*(B11). https://doi.org/10.1029/2007JB005375

Westaway, R. (2002). The Quaternary evolution of the Gulf of Corinth, central Greece: coupling between surface processes and flow in the lower continental crust. *Tectonophysics*, *348*(4), 269–318. https://doi.org/10.1016/S0040-1951(02)00032-X

Wilkinson, M. W., McCaffrey, K. J. W., Roberts, G. P., Cowie, P. A., Phillips, R. J., Michetti, A. M., et al. (2010). Partitioned postseismic deformation associated with the 2009 Mw 6.3 L'Aquila earthquake surface rupture measured using a terrestrial laser scanner. *Geophysical Research Letters*, *37*(10), 1–7. https://doi.org/10.1029/2010GL043099

Wilkinson, M. W., McCaffrey, K. J. W., Roberts, G. P., Cowie, P. A., Phillips, R. J., Degasperi, M., et al. (2012). Distribution and magnitude of post-seismic deformation of the 2009 L'Aquila earthquake (M6.3) surface rupture measured using repeat terrestrial laser scanning: Post-seismic deformation: L'Aquila surface rupture. *Geophysical Journal International*, *189*(2), 911–922. https://doi.org/10.1111/j.1365-246X.2012.05418.x

Wright, T. J., Parsons, B. E., & Lu, Z. (2004). Toward mapping surface deformation in three dimensions using InSAR. *Geophysical Research Letters*, *31*(1). https://doi.org/10.1029/2003GL018827

Zelt, B. C., Taylor, B., Sachpazi, M., & Hirn, A. (2005). Crustal velocity and Moho structure beneath the Gulf of Corinth, Greece. *Geophysical Journal International*, *162*(1), 257–268. https://doi.org/10.1111/j.1365-246X.2005.02640.x

Supplementary Figures

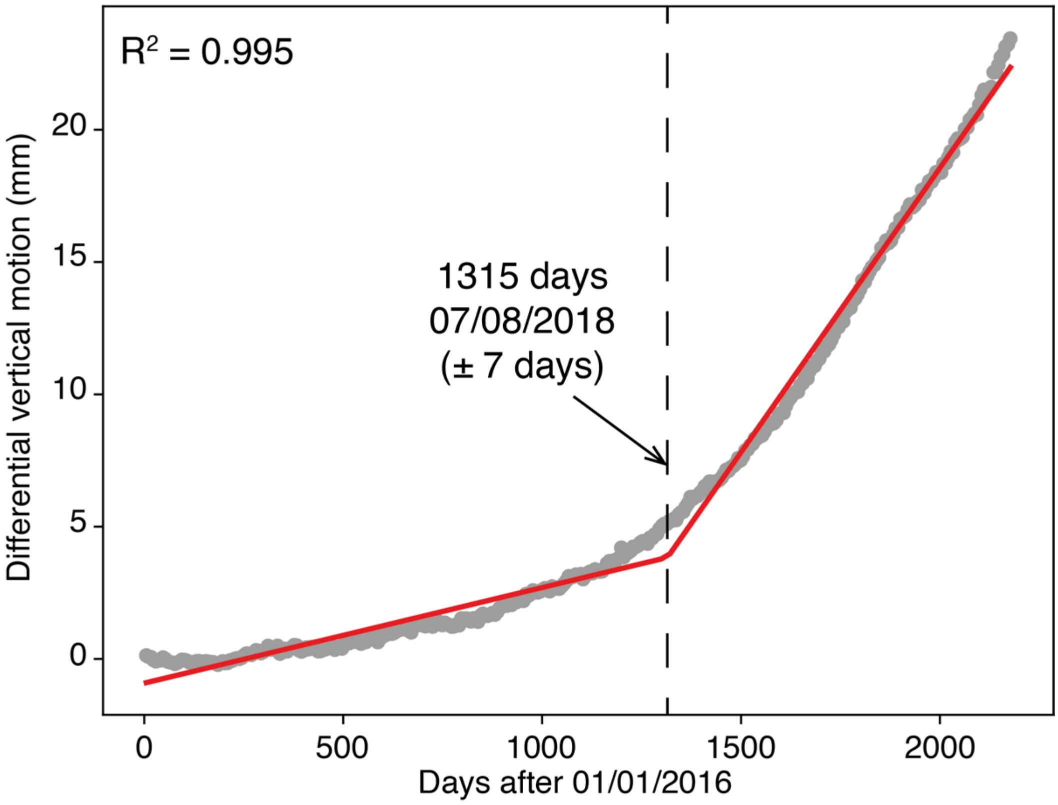

Figure S1. *Results of piecewise linear regression analysis, following* (Pilgrim, 2021). *Assuming only one breakpoint, the best fit breakpoint in the data is at 1315 ± 7 days, which corresponds to a date of 07/08/2018.*

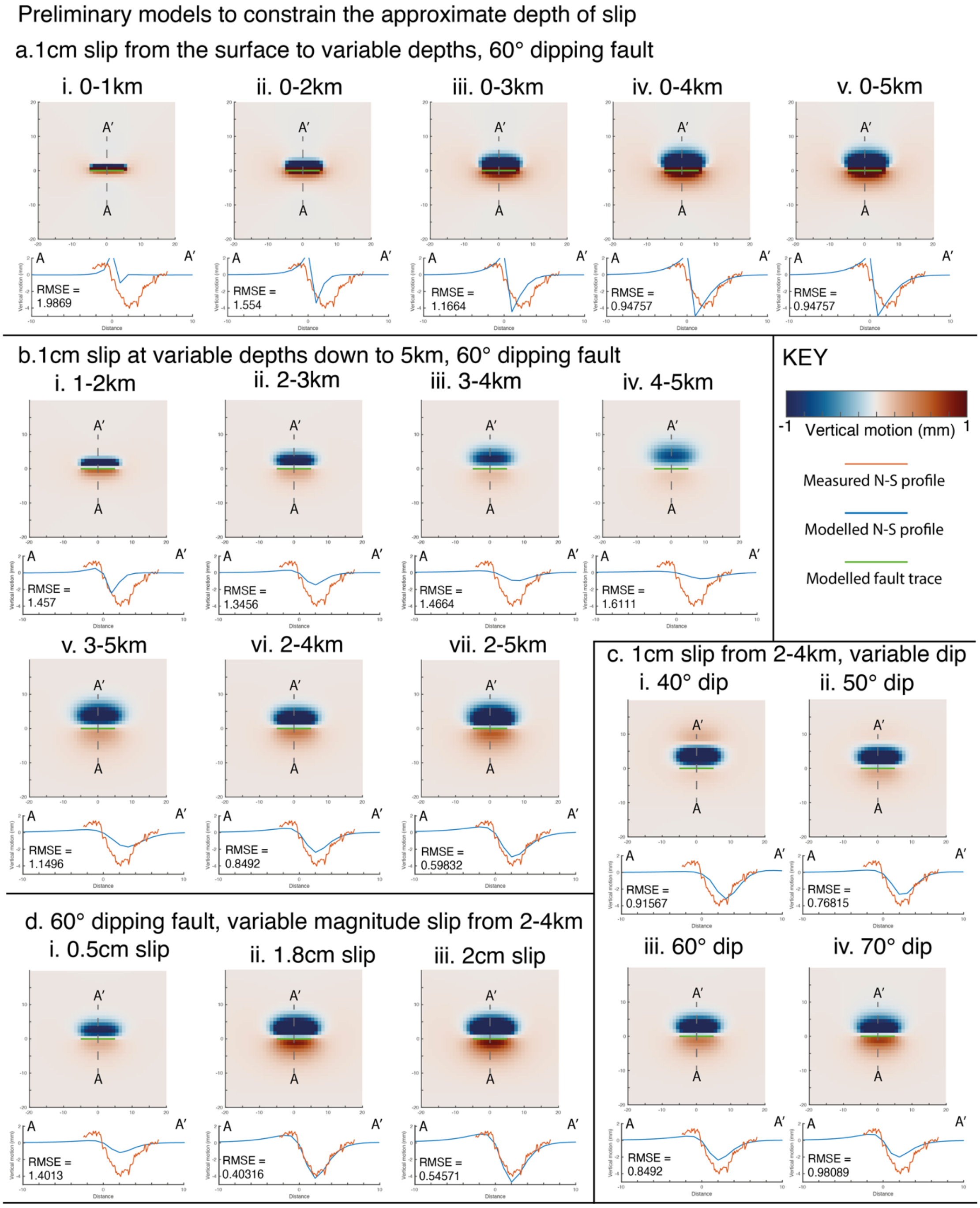

Figure S2. *Elastic-half space modelling to provide constraints on the parameters of shallow aseismic slip. The models are evaluated by comparing the modelled N-S profile (blue line) to the average N-S deformation from the data (orange line, from Figure 2b). The best-fit model is 1.8 cm slip from 2-4 km depth on a fault dipping 60°. This is not a full inversion, which would not be possible given the discontinuous nature of data along the full length of the Pisia-Skinos fault. However, these models can be used to give approximate constraints on the location and magnitude of aseismic slip that we hypothesise is the physical mechanism producing the transient vertical deformation signal observed in the EGMS data.*